How the Presence and Size of Static Peripheral Blur Affects Cybersickness in Virtual Reality

YUN-XUAN LIN and ROHITH VENKATAKRISHNAN, National Chiao Tung University (Taiwan) and Clemson University (USA)
ROSHAN VENKATAKRISHNAN, Clemson University, USA
ELHAM EBRAHIMI, University of North Carolina Wilmington, USA
WEN-CHIEH LIN, National Chiao Tung University, Taiwan
SABARISH V. BABU, Clemson University, USA

16

Cybersickness (CS) is one of the challenges that has hindered the widespread adoption of Virtual Reality and its applications. Consequently, a number of studies have focused on extensively understanding and reducing CS. Inspired by previous work that has sought to reduce CS using foveated rendering and Field of View (FOV) restrictions, we investigated how the presence and size of a static central window in peripheral FOV blurring affects CS. To facilitate this peripheral FOV blur, we applied a Gaussian blur effect in the display peripheral region, provisioning a full-resolution central window. Thirty participants took part in a three-session, within-subjects experiment, performing search and spatial updating tasks in a first-person, slow-walking, maze-traveling scenario. Two different central window sizes (small and large) were tested against a baseline condition that didn't feature display peripheral blurring. Results revealed that the baseline condition produced higher levels of CS than both conditions with a central window. While there were no significant differences between the small and large windows, we observed interaction effects suggesting an influence of window size on "adaptation to CS." When the central window is small, adaptation to CS seems to take more time but is more pronounced. The interventions had no effect on spatial updating and presence, but were detectable when the blurred area was larger (small central window). Lower sickness levels observed in both window conditions supports the use of peripheral FOV blurring to reduce CS, reducing our dependence on eye tracking. This being said, researchers must strive to find the right balance between window size and detectability to ensure seamless virtual experiences.

CCS Concepts: • **Human-centered computing → Virtual reality**;

Additional Key Words and Phrases: Virtual reality, cybersickness, blurring, foveated rendering

Y.-X. Lin and R. Venkatakrishnan contributed equally to this research.

This work was supported in part by the Ministry of Science and Technology of Taiwan under Grant No. 109-2221-E-009-123-MY3.

Authors' addresses: Y.-X. Lin, National Chiao Tung University, No. 1001, Daxue Road, East District, Hsinchu City, Taiwan 300; email: librechat2514@gmail.com; R. Venkatakrishnan, Clemson University, School of Computing, 821 McMillan Rd, Clemson, South Carolina - 29631, USA; email: rohithv@g.clemson.edu; R. Venkatakrishnan and S. V. Babu, Clemson University, School of Computing, 821 McMillan Rd, Clemson, South Carolina - 29631, USA; emails: rvenkat@g.clemson.edu, sbabu@clemson.edu; E. Ebrahimi, Department of Computer Science, University of North Carolina Wilmington, Congdon Hall, 601 South College Road, Wilmington, North Carolina - 28403, USA; email: ebrahimie@uncw.edu; W.-C. Lin, National Chiao Tung University, No. 1001, Daxue Road, East District, Hsinchu City, Taiwan 300; email: wclin@cs.nctu.edu.tw.

1544-3558/2020/11-ART16 $15.00
https://doi.org/10.1145/3419984

ACM Reference format:
Yun-Xuan Lin, Rohith Venkatakrishnan, Roshan Venkatakrishnan, Elham Ebrahimi, Wen-Chieh Lin, and Sabarish V. Babu. 2020. How the Presence and Size of Static Peripheral Blur Affects Cybersickness in Virtual Reality. *ACM Trans. Appl. Percept.* 17, 4, Article 16 (November 2020), 18 pages.
https://doi.org/10.1145/3419984

1 INTRODUCTION

Virtual Reality (VR) technologies have started to see the integration of their applications into the areas of gaming [20], training [22], education [12], therapy [54], and so on. However, even with this continuous permeation of VR into our lives, we are yet to see the technology's widespread adoption. This may largely come down to the issue of cybersickness (CS), which often accompanies VR usage as a side effect. Cybersickness, a malady like motion sickness, is thought to occur when the brain receives mismatched sensory information about motion from multiple senses [47]. These senses often include the visual and vestibular perceptual systems [50]. Other cybersickness researchers adopt a different school of thought, positing that cybersickness is a consequence of the body's failure to maintain postural stability while experiencing new stimuli [49]. This is classically called the "Postural Instability Theory," and recent work on this front has shown that postural stability can predict the likelihood of cybersickness in HMD-based virtual reality simulations [5]. While other theories such as the "Poison Theory," "Rest Frame Theory," and so on, have offered explanations for the manifestation of motion sickness, the "Sensory Conflict" and "Postural Instability" theories remain the most prominent in the research community [48]. As such, in immersive virtual environments (IVEs), CS commonly occurs when the display devices provide visual stimulation to the users wherein they perceive motion.

To minimize the disparity between visual and vestibular perception, high-frame-rate rendering techniques and high-fidelity tracking systems have been adopted, thereby reducing cybersickness [13, 32, 45, 58]. However, such approaches are not always accessible due to resource constraints. Besides, high quality tracking systems are of little use when the physical space in the real world is limited. Another technique commonly used to reduce CS involves reducing the perception of motion through vision. This has been achieved by simply decreasing the users' field of view (FOV) [19, 42], directly snapping moving frames [18, 37, 55], or by using full-screen blurring [8]. While these approaches have successfully mitigated CS, research has shown that they can come at the cost of users' task performance and presence levels [6]. These trade-offs have often been attributed to the reduced scene information available for perception [8, 18, 37, 55]. To avoid such compromises created by employing full-screen visual effects, Nie et al. (2019) proposed the use of a partial blurring approach in a high-speed, race-car scenario [41]. This study predicted users' area of focus using a saliency map [40], and blurred the areas predicted to be unattended to, whose size and location varied dynamically. Toward reducing CS, Carnegie and Rhee [10] adopted a dynamic depth-of-field (DOF) approach, using the object at the center of the users' FOV as the focus target.

While previous studies have focused on dynamically varying the blur region, limited work has explored how the size of a static blurred region of the display periphery affects sickness, and if/how this manipulation affects spatial task performance and presence levels within the IVE. Given that aspects like these are crucial to the VR experience, it is imperative that we understand how they are affected in such scenarios. Furthermore, in comparison to a dynamically varying blurred region, a static peripheral blurred region (fixed foveated rendering (FFR) or peripheral FOV blurring), provides for a much simpler approach to reduce cybersickness, due to requiring no additional resources apart from the rendered images. Additionally, by studying the effects of the size of static blur regions, researchers can eliminate "varying size" as an extraneous influence that accompanies techniques employing dynamic blurring toward the alleviation of CS.

Inspired by previous works that have sought to reduce cybersickness by leveraging blurring [8, 10, 41] and dynamic FOV rendering [19], we aimed at determining how the manipulation of the size of the static foveal region (central full resolution window in FFR) affects sickness, and whether or not this manipulation has trade offs associated with it. Toward this end, we empirically evaluated how two different central window sizes affects CS when peripheral FOV Blurring is applied in a virtual maze scenario. Throughout this article, we use the terms "static peripheral blurring," "peripheral FOV blurring," and "fixed foveated rendering" interchangeably to describe a blurring technique that blurs out the display peripheral region that remains constant with respect to the display screen of the head mounted display. Instead of blackening out the display periphery as done in FOV restriction, peripheral FOV blurring involves blurring out the display peripheral region.

2 BACKGROUND AND RELATED WORKS

2.1 Cybersickness

Cybersickness is often described as the discomfort felt by users while experiencing virtual environments, frequently marked by symptoms such as nausea, sweating, eye strain, dizziness, disorientation, and so on [33]. It usually occurs when users are exposed to visual motion stimuli while remaining relatively stationary in the real world, and is commonly referred to as visually induced motion sickness (VIMS) [30]. According to the "Sensory Conflict Theory," a conflict between the visual and vestibular sensory perceptual systems is created, wherein the former suggests that one is in motion and the latter, otherwise [33]. The "Postural Instability Theory," however, argues that a reduced ability to control postural motion causes motion sickness. In general, VIMS can be seen as a visually induced subset of motion sickness, commonly experienced when traveling in IVEs [23, 35]. The exposure to visual motion stimuli produces a perception of self motion called vection, which is often linked to VIMS, if not a prerequisite [31]. Given this relationship, it is possible to predict cybersickness through visual aspects associated with vection such as optic flow rate, virtual motion velocity, and FOV [34, 43].

Questionnaires: The simulator sickness questionnaire (SSQ) developed by Kennedy et al. [28] is widely used to evaluate the levels of cybersickness induced. The survey is administered twice in a pre and post fashion, thereby allowing to estimate the change in sickness produced as a result of a simulation. The research community has, however, shifted toward administering the SSQ only post test to avoid any possible priming effects. This being said, a number of recent studies such as References [52, 53] continue to administer the SSQ both pre and post test to ascertain the change in sickness produced from a measured baseline. The motion sickness susceptibility questionnaire (MSSQ) is a subjective questionnaire often used as a means of determining how likely an individual is to experience motion sickness [21], and has recently been used as an exclusion criterion for participants in CS studies [4].

Measuring Cybersickness during VR Experiences: The fast motion sickness scale (FMS) was developed to measure cybersickness during stimulus presentation. This 20-point scale requires users to verbally report their sickness levels periodically during the simulation, thus allowing for an in situ measure of cybersickness with the added ability to capture its time course [29]. We used a shortened variant of this scale similar to those outlined in References [52, 53].

2.2 Visual Interventions to Reduce Cybersickness

Several approaches, both loosely and tightly coupled with the visual characteristics of VR experiences, have been employed to reduce cybersickness in the past. The former includes the use of high frame-rate rendering, high quality tracking systems with reduced latency and tracking error, and so on [13, 32, 45, 58]. The latter, however, focuses more on direct visual interventions to reduce CS, and our work seeks to contribute to this knowledge base.

Direct visual manipulations that reduce vection can also reduce cybersickness. This has been achieved by decreasing the FOV (tunneling) [19, 42] or directly snapping moving frames [18, 55]. To snap frames, Farmani et al. simply cut the rotational frames [18]. Other efforts have involved skipping or obscuring translational frames by leveraging virtual teleportation [37, 55] and full-screen blurring [8]. While such efforts have shown promise in alleviating CS, they come with compromises that are concomitant with the full screen nature of these manipulations. These trade offs include reductions in spatial knowledge acquisition, efficacy of task performance, presence levels, and so on [6, 37, 55]. To reduce such compromises, researchers have proposed the use of non full-screen effects. Apropos of this, the authors of Reference [10] adopted a dynamic DOF approach to reduce CS using the object at the center of the FOV as the focus target. Saliency map-based dynamic peripheral blurring effects have also been used to reduce CS in a high-speed race car scenario [41]. With several modern VR applications increasingly adopting lower travel speeds to reduce CS, it may be worthwhile to focus on scenarios involving walking speeds. Other studies have also made use of non full-screen techniques toward CS reduction by dynamically varying visual aspects [9, 19]. While such works involving dynamic blurring based on saliency or depth may have successfully reduced CS, it is plausible that the varying size of the dynamic blurred region may have influenced these observed effects. Since the blur region in such approaches is dynamically determined and is subject to changes in size throughout the experience, there exists an extraneous influence of the changing size of the blur region in alleviating CS. This influence of the size of the blurred region on cybersickness remains relatively unexplored in fully immersive virtual experiences achieved using tracked head mounted displays. In an effort to understand how this size of the blurred region affects sickness, we manipulated the size of a static full resolution central window as an experimental factor in a fully immersive virtual experience involving peripheral FOV blurring.

2.3 Peripheral Blur and Foveated Rendering

Foveated rendering (FR) is a technique that reduces GPU workload by devoting more of the rendering effort to the foveal region, and leaving the non-foveal areas to be rendered in a lower resolution [44]. Peripheral Blurring is one method of FR that blurs the peripheral region to reduce the image quality. FR usually involves an eye tracking component that determines where the peripheral region is, but can also be implemented primitively (FFR) without eye tracking, as in Reference [1]. The peripheral region can hence either involve the periphery of the image that is fixed with respect to the display screen (display periphery) or the periphery of the retinal visual field that is constant with respect to the eye but dynamic with respect to the display screen (retinal periphery). Studies that involve FR, display and retinal peripheral blurring have been characterized by the intention to both improve upon GPU performance, and reduce the detectability associated with them. Efforts on this front have hence largely focused on implementing novel algorithms toward achieving improved system throughput. Along these lines, a kernel-based log-polar mapping algorithm was designed to enable a parameterized trade off between visual quality and rendering speed for FR [36]. Swafford and his colleagues proposed different quality degradation methods including reduced rendered pixel density, ambient occlusion, tessellation, and foveally selective ray-casting toward examining how these techniques compare in GPU performance and user detectability [51]. The potential benefits of peripheral blurring have been addressed by work conducted by Hillaire et al. (2009), who introduced a model of dynamic visual blurring based on two types of blur effects, namely, depth of field blurring (blurring of objects related to focalization) and peripheral blurring (blurring the periphery of the field of view) . The authors developed a technique to automatically compute focal distance while provisioning temporal filtering of the focal distance toward simulating the phenomenon of accommodation [24]. They were able to show that the activation of visual blur effects did not seem to impair gamers' performance during multiple sessions of a multiplayer first person shooter game played on a desktop. Furthermore, it was observed that users prefer peripheral blurring being added, because they felt that it increased the realism associated with the experience. This work, however, did not probe into the impact of peripheral blurring on cybersickness in fully immersive virtual experiences achieved using tracked head mounted displays thus opening an avenue for research that we intended to pursue.

The literature has remained relatively silent on the effects of the size of the foveal/peripheral blur region on cybersickness. Nevertheless, studies in this realm continue to concentrate on how noticeable and preferable

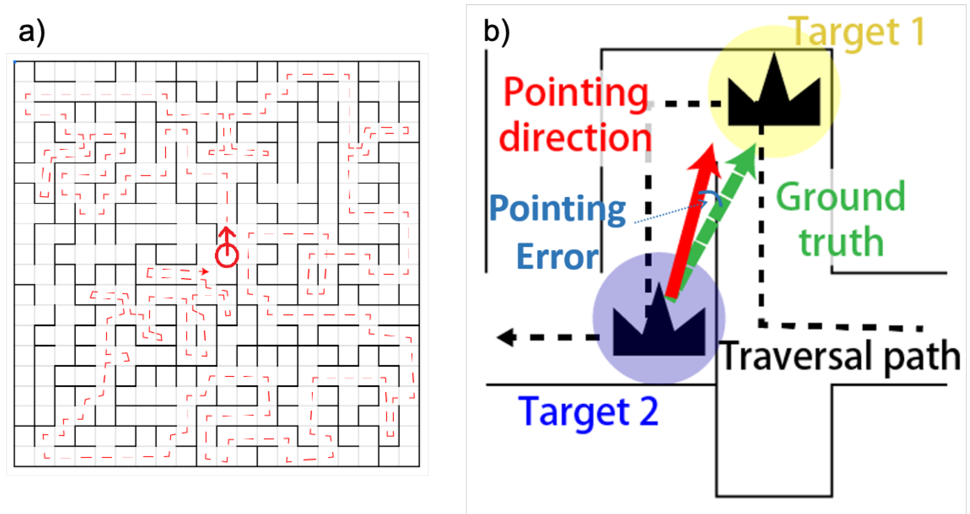

Fig. 1. (a) Virtual maze layout with predefined traversal path. (b) Spatial orientation task trial using target objects.

different peripheral window sizes are, toward coming up with threshold values of the sizes that users tolerate most. Weier et al. (2016) adopted different foveal region sizes and discovered that users cannot reliably differentiate between full and foveated rendering when foveal regions are larger than 10° [56]. Hsu et al. [26] evaluated the detectability of foveally rendered images with different central window sizes and peripheral resolutions. They found that the participants barely noticed the presence of FR when implemented with an eccentricity of 7.5°+ and a peripheral region resolution of 540p+. Other work has shown that users can tolerate up to 2× larger blur radius before detecting differences from a non-foveated ground truth [44]. While Oculus Go [1] employs fixed foveated rendering with a static foveal region, little is known about the effects of the size of this foveal region on aspects of the virtual experience.

As such there is limited work that has explored the role of foveal region size on cybersickness in IVEs. We attempt to bridge this gap by examining how the presence and size of a static, blurred display-peripheral region (therefor a static central window) in peripheral FOV blurring affects CS and other aspects associated with immersive virtual experiences.

3 SYSTEM DESCRIPTION

3.1 Equipment and Virtual Environment

To build the virtual environment for our study, we used a commodity HMD, HTC Vive Pro,[1] and a computer equipped with an Intel i7-8700 processor, 32 GB of RAM, and an NVIDIA RTX 2080 graphics card. The HTC Vive Pro HMD had an FOV of 110° with a frame refresh rate of 90 Hz. The HTC Vive controllers were used to move around and perform tasks in the IVE.

We built a 20×20 block (40×40 m) maze (Figure 1(a)) using the Unity game engine's assets and meshes. Realistic textures and shaders were applied to increase both the realism and optic flow associated with the scene. The maze contained object models that were used in the tasks described in Section 4.3.

Participants could translate and rotate within the IVE using the HTC Vive Controller. This was programmed to afford rotation at 18°/s and translation at a maximum speed of 0.9 m/s, resembling real world walking speeds [14]. Participants were also free to move and rotate their heads during the simulation, allowing them to observe

[1] http://www.vive.com/us/product/vive-pro.

details when in motion. A predefined path was constructed by sequentially placing 100 red balls along a specific path in the maze. Participants moved along this path, locating and collecting each ball one after another. They were seated on a fixed chair during the experience, thus increasing visual-vestibular mismatch. On average, it took between 15 and 20 minutes to completely traverse the maze.

3.2 Peripheral FOV Blur

We generated a peripheral blur effect by applying a Gaussian blur filter in the display peripheral region [44], and provisioned a central image area with full resolution. We call this central non-blurred area, the *central window*. This is similar to the foveal region in fixed foveated rendering. To avoid any possible perceptual/CS effects associated with dynamically varying central window positions, we fixed the central window at the center of the FOV, just like how fixed foveated rendering is implemented in the Oculus Go [1]. As mentioned earlier, the image inside the central window was displayed with the original resolution (615 PPI) as provided by the Vive pro headset. The resolution of the image outside the central window was reduced by applying a Gaussian blur filter of kernel size 13. There hence was little to no reduction in the frame rate due to our visual effect simulation. Given that the frame rates under different conditions were almost identical (110 fps), there was no differential influence of frame rate on cybersickness across the experimental conditions.

We additionally used a soft-edged resolution restrictor to avoid distraction caused by the hard-edged cutouts between the blurred and non-blurred regions. As shown in Figure 2(a), the restrictor had an inner and outer circle. For pixels between the two circles, the kernel size of the Gaussian filter linearly decreased from 13 (outer circle) to 1 (inner circle). Within the inner circle (central window), no blurring was applied.

4 EXPERIMENT DESIGN

4.1 Research Questions

We specifically aimed at answering the following research question: "**How does the size of a static full resolution central window with peripheral blurred outer regions, affect cybersickness in IVEs?**" Downstream of this, we were interested in observing if the window size affects spatial knowledge acquisition and presence levels associated with the virtual experience. We operationalize cybersickness, spatial knowledge acquisition and presence using measures described in Section 4.6.

4.2 Experimental Conditions

In pursuit of our research interests, we conducted a three-session within-subjects study manipulating the size of the central window across three experimental conditions: (1) Normal Viewing (NV) (no peripheral blur effect applied to image); (2) Large Window (LW) (large full resolution central window); (3) Small Window (SW) (small full resolution central window). See Figure 2. Each session was conducted on a separate day leaving a one day gap between two consecutive sessions. Since we blurred the peripheral region outside the central window, a larger central window implies a smaller blurred region and vice versa.

The sizes of the central windows used in this study were determined based on previous detectability works [26, 56], and the distribution of gaze amplitudes [17]. Table 1 lists details associated with the central window sizes, and Figure 2 depicts the scene in the three conditions. To counterbalance for any possible occurrences of order effects, we had six different condition orders, each of which was a permuted order of the three conditions. The position of the central window was fixed at the center of the image in all conditions. All three conditions featured the same virtual scene.

4.3 Tasks

We designed two tasks in the IVE: a search and a spatial orientation task. The search task was used to guide participants through the maze along a predefined path, while the spatial orientation task was used to measure

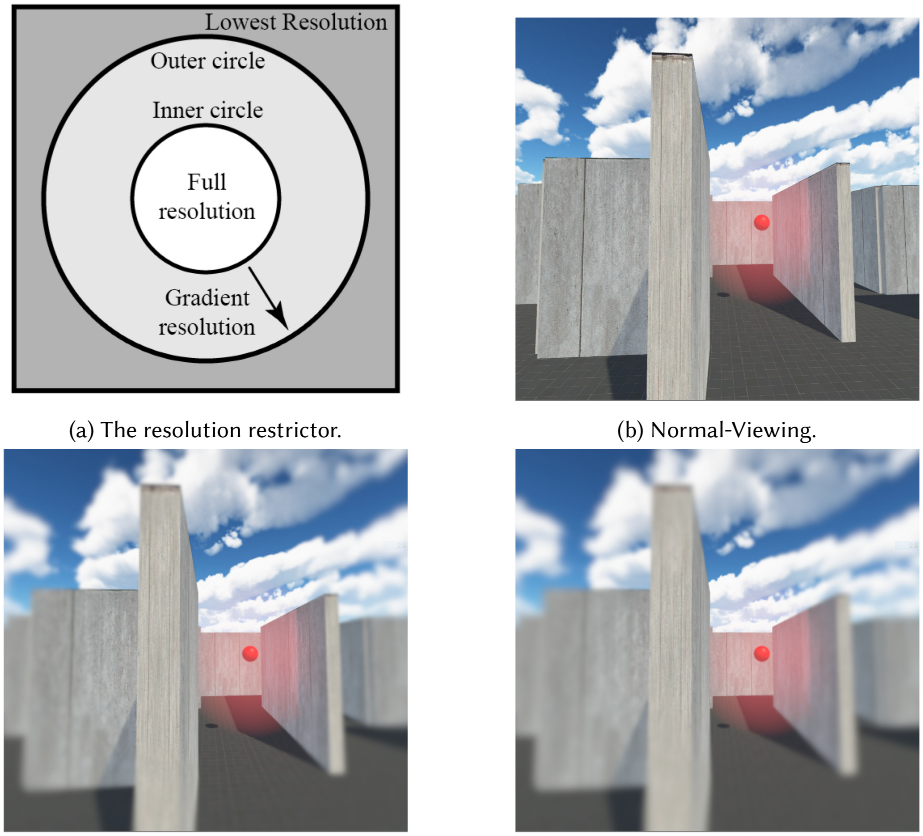

(a) The resolution restrictor.

(b) Normal-Viewing.

(c) Large-Window.

(d) Small-Window.

Fig. 2. (a) Soft-edged resolution restrictor. (b) Virtual scene without peripheral blur, and (c, d) Virtual scene with different central window sizes.

Table 1. Size Sets of Central Window

Radius of the central window		Inner circle	Outer circle
Small	Screen size ratio	0.1	0.3
	Pixels per eye	114 * 160	432 * 480
	Visual angle	15	30
Large	Screen size ratio	0.17	0.37
	Pixels per eye	245 * 272	533 * 592
	Visual angle	28	35

spatial knowledge acquisition. Both tasks also served to engage participants. Participants had to perform the spatial orientation task while they were guided through the maze. To lower cognitive workload, we made the tasks simple and confirmed this through pilot studies. The details of each task are discussed below:

Search Task: Participants were told to locate and collect red balls that would appear in the maze, by touching them with the controller. At any given time, there was only one ball in the scene. Upon collection, the ball disappeared and another ball was spawned nearby, making it easily discoverable. A total of 100 red balls were sequentially spawned at predefined positions along a predefined path, thereby guiding participants through the maze.

To keep the visual stimuli consistent across conditions, we used the same predefined path in all conditions (Figure 1(a)). However, this path was reversed (opposite direction) between sessions to ensure that no two continuous sessions had the same exact path. The path was designed to make participants perform rotations and translations in the maze, and to induce cybersickness through their virtual movements. From both the pilots and our formal study, the majority of participants reported that they could hardly remember the path they had experienced in their previous session(s). This was likely due to the one-day-break between sessions, which was employed to eliminate any possible learning or carry over effects.

Spatial Updating Task: A spatial updating task was introduced to measure participants' spatial knowledge acquisition [55] and to induce more rotational movements. This task included 20 trials. Every trial involved one object that would appear in two different locations in the maze, and at two distinct times (see Figure 1(b)). The object was first spawned at a particular location, highlighted in yellow. Participants made note of the object and its location, because they had to recall and point toward this location when they encountered it again later at a different location in the maze (this time highlighted in blue). An audio clip was invoked when subjects encountered the object for the second time (highlighted in blue), asking them to point toward the location where they first saw the object (highlighted in yellow). It was ensured that the number of turns between the first and second appearance of the object was less than 4, making it reasonable enough for trials to transpire within minutes. Furthermore, to reduce the cognitive load associated with memory, it was ensured that no two trials overlapped. A total of 20 different objects were used for the trials, all of which were spawned along the predefined traversal path described earlier.

4.4 Participants

We recruited 35 participants for this Institution Review Board (IRB)-approved study. Their ages ranged from 19 to 27 (average age = 22.7 years). Most of the participants were college or graduate students who majored in engineering or sciences. All participants had normal or corrected to 20/20 vision. Participants with less than 6 h of sleep prior to the experiment were excluded from participating in the study. Individuals that indicated any feelings of fatigue and body pain were also excluded. After exclusion, we had a total of 30 participants (15F,15M).

4.5 Procedure

In each session, participants were greeted and asked to read and sign a consent form (informed consent) upon arrival. After consenting to participate in the study, participants filled out a demographics questionnaire that included information about their backgrounds and experience with VR, 3D movies and video games. Following this, they were administered the motion sickness susceptibility questionnaire (MSSQ) [21] after which, they were briefed about the experiment and the tasks that they were required to perform. In a training phase, they were then acclimated to the VR interaction metaphor. This training, however, took place in the real world (not in VR) to avoid any carryover effects of cybersickness that could have surfaced through a VR training phase. Each subject was then randomly assigned to one of the six condition orders, and one of the two path directions (default path and its reverse), which have been described earlier. Each of the three sessions (one condition per day) was conducted on a separate day with a one-day break between sessions in a manner similar to References [15, 16]. We describe the procedural sequence in each session below:

(1) In each session, subjects first filled out a pre-experiment simulator sickness questionnaire (SSQ) [28].
(2) Following this, participants were seated on a fixed chair and were free to move and rotate their heads and shoulders arbitrarily. They were, however, instructed to remain seated during the course of the VR experience and had to move and rotate virtually with the aid of the controller. To avoid priming participants,

the instructions did not mention anything about the simulation making them sick. However, they were told that they could quit at any time.

(3) Participants were also instructed to verbally report their levels of physiological discomfort on a ten point scale whenever they heard an audio clip question that was played by the simulation, in a manner similar to References [19, 52, 53]. This audio clip question was automated to play every two minutes, and was phrased as follows: *"On a scale from one to ten, where one represents most comfortable and ten represents most uncomfortable, how do you feel?"*

(4) Following these instructions, participants began the simulation where they had to travel in the virtual maze, completing the search and spatial orientation tasks. The simulation ended when participants got sick and could no longer continue (verbal indication or reported comfort score of 10) or when they completed both tasks.

(5) After the simulation, subjects filled out the SSQ [28] again, the Igroup Presence Questionnaire (IPQ) [27], and engaged in a semi-structured interview that probed into details associated with the simulation, and ended with debriefing. The end of the interview marked the end of the session.

4.6 Measures

4.6.1 Cybersickness. We used two measures to assess the levels of cybersickness induced. The first was the computed difference scores between the Post and Pre instances of the SSQ questionnaire described in Reference [28]. Our second measure of cybersickness involved periodic verbal reports of a 10-point-scale-based score of discomfort that was obtained from the participants every two minutes during the simulation. This provided a means to ascertain cybersickness trends within a session using a repeated measure as done in References [52, 53].

4.6.2 Task Performance. To explore how the size of the central window affects participants' performance on spatial knowledge acquisition in the IVE, we measured the following:

Search time: The time interval between a participant collecting two red balls.

Error in spatial updating: When the spatial updating task (see Section 4.3) was being performed, we recorded each participant's pointing vector and the ground truth vector to the actual target location (highlighted in yellow). The angular difference between these two projected vectors (the pointing and ground truth vectors) is defined as the error in spatial updating (see Figure 1(b)).

4.6.3 Presence. To measure the levels of presence experienced during the simulation, we used the IPQ presence questionnaire [27].

4.6.4 Subjective Perceptions across Sessions. We conducted semi-structured interviews after each session in an effort to qualitatively understand how participants experienced and perceived the different conditions. We intended to uncover both participants' perceptions of the images in the conditions as well as any differences they may have noticed between sessions. After the third session, the interview included a question that asked participants to compare their experiences across sessions. We made sure to avoid mentioning anything related to the visual manipulations performed to prevent participants from being primed. The interviews allowed us to ascertain if subjects noticed anything "out of the ordinary" in each condition.

5 RESULTS

We discuss the results of our analyses in this section. With the possibility of participants adapting to the stimuli over different sessions, we included the order of the sessions as a factor in our statistical analyses.

5.1 Discomfort Score

To analyze discomfort, we plotted participants' discomfort scores at different times during the sessions. Some participants terminated the session early, indicating a discomfort score of 10 (Figure 3(a)). The number of

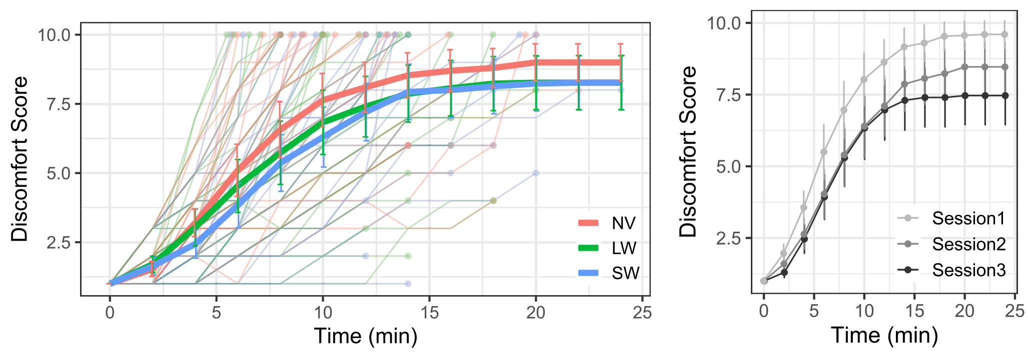

(a) Curves of conditions.

(b) Curves of session orders.

Fig. 3. (a) Average discomfort score trends for each condition. Error bars represent 95% confidence intervals. Data points indicate completion/termination of session. (b) Average discomfort trends for each session.

Table 2. The Mixed Model ANOVA Results at Each Time Point We Recorded the Discomfort Score

Time Point	t_1	t_2	t_3	t_4	t_5	t_6	t_7	t_8	t_9	t_{10}	t_{11}	t_{12}
Condition	NS	NS	NS	NS	NS	NS	NS	NS	NS	NS	NS	NS
Session[a]	$F = 5.813$ $p = 0.004$ $\eta^2 = 0.121$	$F = 5.266$ $p = 0.007$ $\eta^2 = 0.101$	$F = 4.218$ $p = 0.018$ $\eta^2 = 0.086$	$F = 3.463$ $p = 0.036$ $\eta^2 = 0.071$	$F = 3.616$ $p = 0.031$ $\eta^2 = 0.074$	$F = 3.766$ $p = 0.027$ $\eta^2 = 0.078$	$F = 4.889$ $p = 0.009$ $\eta^2 = 0.095$	$F = 5.265$ $p = 0.007$ $\eta^2 = 0.101$	$F = 7.382$ $p = 0.001$ $\eta^2 = 0.134$	$F = 7.190$ $p = 0.001$ $\eta^2 = 0.130$	$F = 7.515$ $p = 0.001$ $\eta^2 = 0.135$	$F = 7.515$ $p = 0.001$ $\eta^2 = 0.135$
Condition[b] × Session	NS	NS	NS	NS	NS	NS	NS	$F = 2.526$ $p = 0.046$ $\eta^2 = 0.097$	$F = 3.075$ $p = 0.020$ $\eta^2 = 0.112$	$F = 3.048$ $p = 0.021$ $\eta^2 = 0.110$	$F = 3.132$ $p = 0.018$ $\eta^2 = 0.112$	$F = 3.132$ $p = 0.018$ $\eta^2 = 0.112$

a: $F = F(2, 81)$, b: $F = F(4, 81)$, NS: no significant difference.

discomfort scores sampled from each participant was hence different, requiring us to use the last reported score for the remaining samples if any. The duration of the longest session was 24 min, implying there were 13 discomfort score samples (including the zeroth sample).

5.1.1 Discomfort Score at Each Time Point. The discomfort scores with different conditions were averaged at each time point we recorded them. We applied a mixed model ANOVA at each time point to investigate the effect of condition (within-subject factor) and session order (between-subject factor) on discomfort score. As shown in Table 2, there was no significant main effect of condition on the discomfort scores. A significant main effect of the session order from times t_1 to t_{12} was observed. Additionally, a significant interaction effect between condition and session order from times t_8 to t_{12} was found. Except for times t_5 and t_6, Bonferroni pairwise comparisons revealed that the discomfort score in Session 3 was significantly lower than in Session 1, $p < 0.05$.

We conducted a block analysis to look into the interaction effect from times t_8 to t_{12}. In the NV condition (Figure 4(a)), there was no significant difference between sessions. In the LW condition (Figure 4(b)), the discomfort profile of Session 1 grows faster than Sessions 2 and 3. Tukey's HSD tests showed that the discomfort score in the LW condition at time t_9 in Session 1 ($M = 10.0$, $SD = 0.00$) was significantly higher than the same in Session 3 ($M = 7.3$, $SD = 2.54$). In the SW condition (Figure 4(c)), the discomfort profile of Session 3 was lower than Sessions 1 and 2. Tukey's HSD pairwise comparisons revealed that for the SW condition from times t_8 to t_{12}, the discomfort scores in Session 3 were significantly lower than both Session 1 ($p < 0.01$) and Session 2 ($p < 0.05$). In Session 3, from times t_8 to t_{12}, the discomfort scores were significantly lower in the SW condition than in the NV condition ($p < 0.05$).

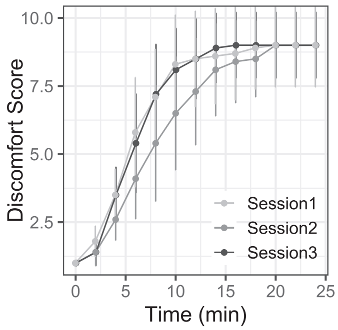

(a) In NV.

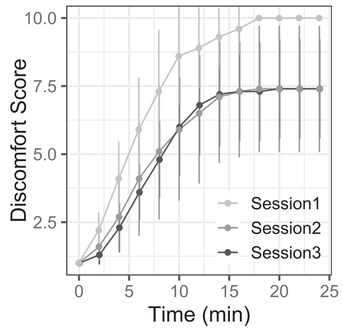

(b) In LW.

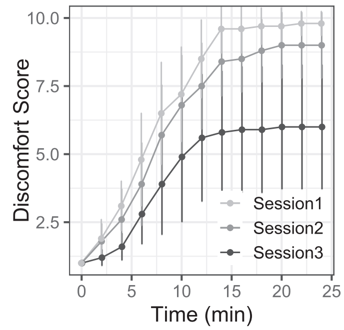

(c) In SW.

Fig. 4. Average discomfort score trends over sessions for each condition.

Table 3. Logarithmic Regression Model Predicting Discomfort Score

Predictor	**B**	**SE**	**t**	**p-value**
Intercept	0.976	0.383	–	–
Condition	−0.368	0.085	−4.308	<0.001***
Log(Time)	2.613	0.147	17.760	<0.001***
Condition × Time	0.016	0.008	2.037	0.041*

*: $p < 0.05$, **: $p < 0.01$, ***: $p < 0.001$.

Table 4. The Emmeans Difference Table for Pairwise Comparison of the Regression Result in Table 3

	emmean	SE	t	p-value
NV − LW	0.538	0.171	3.147	0.004**
NV − SW	0.736	0.171	4.309	<0.001***
LW − SW	0.198	0.171	1.161	0.476

*: $p < 0.05$, **: $p < 0.01$, ***: $p < 0.001$.

5.1.2 Regression Models of Discomfort Score Growth. Multiple regression analysis was used to determine if the slopes and intercepts differed between viewing conditions on the predicted discomfort scores. Multiple regression has been preferred in experiment protocols in which we need to predict a continuous dependent variable (discomfort scores) from both a continuous independent variable (time), a categorical variable (condition), and the interaction between the two, in a manner similar to References [15, 16, 38]. Also, slopes and intercepts given by the regression techniques are more useful than other descriptive statistics, such as session means and signed errors, as they describe the function that predict the participants' indicated discomfort from time and condition. We adopted linear, logarithmic, and logistic regression to fit a model for discomfort score, using conditions (coded as $1 = NV$, $2 = LW$, $3 = SW$) and time (measured in minutes) as predictors.

Entire session: Based on the R^2 value and the S.E. of the estimate, the logarithmic model was chosen as the best-fit regression model. A significant regression equation was found ($F(3, 1166) = 457.5, p < 0.001$), $R^2 = 0.541$ and S.E. = 2.385. The predicted discomfort score was equal to:
0.976 - 0.368 (CONDITION) + 2.613 (log(TIME)) + 0.016 (CONDITION × TIME). See Table 3, Figure 5(a). The time of interaction effect was centered. Pairwise comparisons with the estimated marginal means (emmeans)

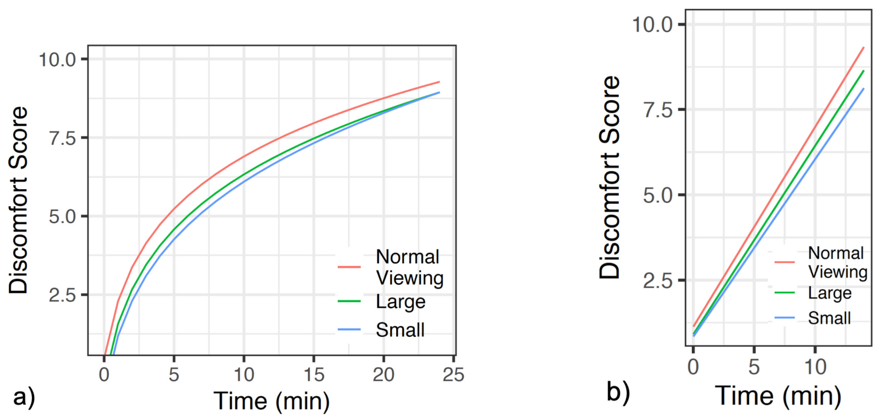

Fig. 5. Predicted discomfort curve of (a) entire session and (b) beginning phase with the best-fit regression model.

Table 5. Linear Piecewise Regression Model Predicting Discomfort Score at the Beginning Phase

Predictor	**B**	**SE**	**t**	**p-value**
Intercept	1.258	0.404	–	–
Condition	−0.373	0.102	−3.641	<0.001***
Log(Time)	0.617	0.048	12.683	<0.001***
Condition × Time	−0.033	0.022	−1.468	0.142

*: $p < 0.05$, **: $p < 0.01$, ***: $p < 0.001$.

Table 6. The Emmeans Difference Table for Pairwise Comparison of the Regression Result in Table 5

	emmean	SE	t	p-value
NV – LW	0.453	0.205	2.205	0.071
NV – SW	0.747	0.205	3.639	<0.001***
LW – SW	0.294	0.205	1.434	0.324

*: $p < 0.05$, **: $p < 0.01$, ***: $p < 0.001$.

are shown in Table 4. The differences between NV and the other two conditions were significant. However, there was no significant difference between LW and SW, indicating that peripheral blurring reduced cybersickness.

Beginning phase: We sampled discomfort scores from times t_0 to t_7 and adopted piecewise regression to find a best-fit model of the beginning phase of the session. A significant linear regression model was found ($F(3, 716) = 304.8$, $p < 0.001$), $R^2 = 0.560$, S.E. = 2.247. The predicted discomfort was equal to: **1.258 − 0.373(CONDITION) + 0.617(TIME) − 0.033(CONDITION × TIME)**. See Table 5 and Figure 3(b). Pairwise comparisons with emmeans revealed that the SW condition was significantly different from the NV condition (Table 6).

To investigate adaption to CS over session, we fit the regression models with conditions, order of sessions, and time as predictors. The logarithmic model was chosen as the best-fit model and a significant regression equation was found ($F(7, 1162) = 250.6$, $p < 0.001$), R^2=0.601, S.E.=2.162. The predicted discomfort score was equal to:

Table 7. The Logarithmic Regression Model Predicting Discomfort Score, Considering the Effect of Session Order

Predictor	B	SE	t	p-value
Intercept	0.755	0.601	–	–
Condition	0.962	0.210	4.564	<0.001***
Session	0.533	0.210	2.529	0.011*
Log(Time)	2.242	0.172	13.019	<0.001***
Condition × Session	−0.664	0.097	−6.811	<0.001***
Condition × Time	0.076	0.013	5.734	<0.001***
Session × Time	0.047	0.013	3.557	<0.001***
Condition × Session × Time	−0.041	0.007	−5.513	<0.001***

*: $p < 0.05$, **: $p < 0.01$, ***: $p < 0.001$.

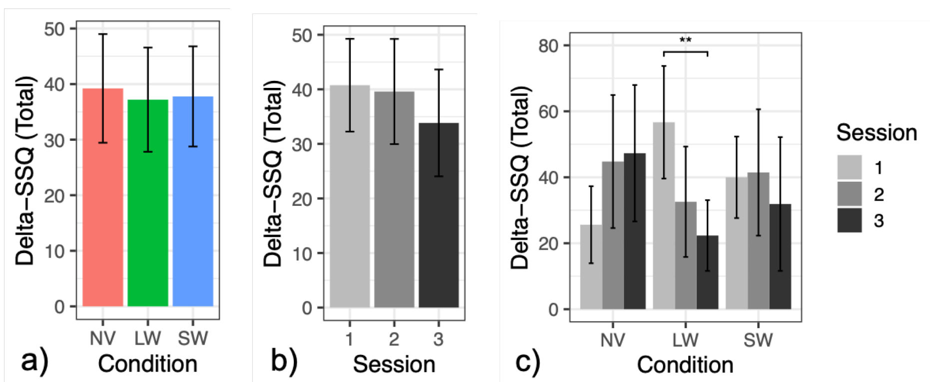

Fig. 6. Delta SSQ broken by (a) condition, (b) session, and (c) condition and session. Error bars represent 95% CI. "**" denotes $p < 0.01$.

0.755 + 0.962(CONDITION) + 0.533(SESSION) + 2.242(log(TIME)) − 0.664(CONDITION × SESSION)+0.076 (CONDITION × TIME) + 0.047(SESSION × TIME) − 0.041(CONDITION × SESSION × TIME). See Table 7. Significant interaction effects revealed an influence of condition on adaptation to CS over sessions.

5.2 Delta between Pre- and Post-SSQ Scores

We computed difference scores in the SSQ to determine the amount of CS induced; i.e., *Delta-SSQ* = *Post-SSQ* − *Pre-SSQ*. Using a mixed model ANOVA, we observed that there was no significant main effect of condition or session order. However, we found a significant interaction effect between them, $F(4, 81) = 3.887$, $p = 0.006$, $\eta^2 = 0.158$.

We conducted a block analysis looking into the interaction effect of session order and condition. Tukey's HSD pairwise comparisons revealed that in the LW condition, the *Delta-SSQ* score in Session 3 ((M = 22.33, SD = 14.99) was significantly lower than in Session 1 (M = 56.67, SD = 23.85), $p = 0.003$ (see Figure 6(c)). However, no significant differences were observed in the NV and SW conditions. With regards to conditions with same session order, Session 1's *Delta-SSQ* scores in the LW condition (M = 56.67, SD = 23.85) were significantly higher than the NV condition (M = 25.60, SD = 16.32), $p = 0.003$.

5.3 Number of Early-Termination (ET) Participants

The number of participants that terminated early was lower in Session 2 (19/30 users) and Session 3 (13/30 users) than in Session 1 (27/30 users). This seems to suggest that frequent exposure to the same scenario may be useful in reducing CS, but more research is needed to confirm this.

5.4 Task Performance and Presence

There were no significant effects found on the average search time of objects, accuracy of spatial updating, and the presence scores.

5.5 Interviews

The data from our interviews shed some light on users' perceptions of the conditions. While about half of the participants indicated that they perceived differences in the image quality across sessions, they were not, however, able to pinpoint and explain what exactly those differences were. Only a few of these participants were confident of what they felt those differences were. Nevertheless, several of these participants commented that they noticed something different with the image quality in the SW condition. This observation was not as pronounced in the LW condition, suggesting that small central windows are more detectable than larger ones. This is likely because the smaller central window had a larger peripheral blur region. Overall, most participants preferred the SW and LW conditions that had central windows more than the NV condition, likely owing to discomforts caused in the NV condition.

6 DISCUSSION

The statistical analyses pertaining to the discomfort scores across entire sessions (Table 3) revealed that there was a significant effect of condition on discomfort scores. Moreover, the pairwise comparisons listed in Table 4 seem to suggest that the introduction of a static central window reduces the sickness experienced regardless of whether the window is small or large. However, we observed no difference between the small and large windows in terms of their effects on sickness, suggesting that the size of the central window does not seem to affect sickness for the two sizes tested in this study. From these results, it seems that the introduction of a static central window with blurred display peripheral regions reduces CS. This aligns with work that has shown that peripheral blurring reduces CS [8], and possibly occurs because vection is stronger when produced by visual stimuli in the peripheral area compared to the central visual area [25]. Moreover, eye gaze behaviors differ in IVEs rendered with foveated and fixed FOV restrictors, wherein the latter confines users' eye gaze to the center of the FOV, possibly explaining why both central window conditions in this study produced lower levels of CS [2]. The analysis of the discomfort scores obtained during beginning phase before participants terminated (see Tables 5 and 6), revealed that there was a significant difference between the discomfort scores reported in the NV and SW conditions. It was found that a small static central window was associated with slower increases in sickness when compared to a visual scene rendered without any peripheral blurring (NV). This can be observed in Figure 5 as the beginning phase is marked by linear profiles followed by which the curves tends to plateau.

The analyses carried out in this study led to some interesting findings on adaptation to cybersickness. We found significant interaction effects between condition and session order on the computed Delta SSQ scores as well as the discomfort scores. From the SSQ results (Figure 6(c)), we observed that the LW condition exhibited trends showing significant reduction in sickness levels over sessions. This trend, however, did not occur in the NV condition. A sort of similar pattern was observed in the curve profiles of the discomfort scores (Figure 4), where the LW condition was associated with significantly higher sickness scores in the first session compared to other two sessions. Additionally, we observed that the curve profile of the third session in the SW condition was considerably lower than that of the first and second sessions. Taking these results together, it seems that introducing static central windows (FFR) could help improve users' adaptation to CS. With respect to window size, we observed that adaptation takes place early when the central window is large, but happens later and stronger when the central window is small. Overall, these findings seem to indicate the possibility of an influence of the central window size on users' adaptation to CS over sessions. However, more work is needed to thoroughly investigate this phenomenon.

With respect to spatial updating, our data revealed that central window sizes had no significant effect on pointing errors and search times. However, from a sickness perspective, this yields a rather interesting takeaway. Using our static peripheral FOV blurring technique, we were able to successfully mitigate CS without any reduction in the levels of spatial awareness and presence. These results address concerns discussed by Reference [55] who showed that skipping translation frames can reduce CS while inadvertently trading off spatial knowledge accuracy. In contrast to Reference [55] that employed jumping as the travel metaphor, our work involved users traveling at slow walking speeds with continuous control over their self motion. It is hence possible that our virtual scenario was conducive to accurately perceive space due to the simplicity of tasks and the virtual travel metaphor employed. This aligns with work showing that the mode of locomotion affects spatial awareness [7, 11, 37]. Furthermore, it seems to be the case that the peripheral FOV blurring technique used in this study did not significantly remove information relevant to spatial localization. This could help explain why no differences were found between the conditions with respect to spatial updating. Since this technique involves a blurred display periphery, it still preserves and presents information needed for spatial updating. The same, however, cannot be said of FOV restriction techniques where the display periphery is blackened out, thus removing information relevant to spatial localization. This may be a reason as to why some studies such as [3, 39, 46, 57] have found FOV restriction to negatively impact spatial navigation and performance in virtual environments. There hence may be merit in employing peripheral FOV blurring toward the reduction of CS without negatively impacting spatial updating.

It may be useful for VR developers to consider static peripheral blurring when creating applications that involve repetitive tasks like those used in therapy, training, exploration, and so on. In the debriefing interviews, we found that a considerable number of users noticed reduced image quality when a small central window was used, making it important for researchers to find the right balance between central window size and detectability, in their pursuits of CS reduction. Determining this sweet spot can hence allow researchers to conduct controlled studies involving window manipulations without affecting users' spatial knowledge, presence, and perceptions of image quality. The data from the interviews also revealed that subjects preferred conditions that featured peripheral blurring and this is consistent with results obtained by Reference [24] who reasoned that increased realism was a likely cause for this observation. We believe that this preference for the addition of peripheral blurring could additionally be explained by the lower amounts of sickness experienced as a result of this intervention. However, the tolerance for blurring the display periphery may be contingent on the type of task involved in the virtual experience. For instance, in a first person shooter game, a heightened attention to the periphery could be an inherent aspect of the experience that determines how well users perceive the experience, and how successful they are at performing the tasks involved. In such scenarios, peripheral FOV blurring need not be tolerated to the same degree as in experiences like the one employed in this study, wherein attention to the periphery may not be as crucial. While Hillaire and his colleagues found no such negative effects of peripheral blurring in desktop virtual experiences, more work is required to determine if the same holds in the context of fully immersive virtual environments achieved using tracked head mounted displays. Our work also serves to show that static peripheral blurring can help in alleviating CS without the need for resource-intensive, gaze-contingent eye tracked components.

7 CONCLUSION AND FUTURE WORK

In this work, we examined how the size of static central windows with peripheral FOV blurring affects CS in a slow-walking virtual maze scenario. Using a three session within subjects design, we empirically evaluated the effects of two central window sizes (small and large) on CS compared to a baseline condition with no peripheral blurring. Results revealed that the baseline condition produced higher levels of sickness than either condition involving a central window. While we observed no significant differences between the two central window sizes, we found significant interaction effects suggesting an influence of window size on adaptation to CS. Large central windows can lead to early adaptation to CS, while small windows seem to have a delayed but stronger effect. Interestingly, users' spatial awareness and presence levels were not affected by the intervention, thus supporting the use of this technique toward reducing sickness without having to compromise the VR experience. The lower levels of CS observed in the experimental conditions shows promise for the use of peripheral FOV blurring, without resource intensive eye tracking, toward the reduction of both GPU workload as well as CS. In future work, we aim to investigate how the geometry (shape) of the central window affects CS. Specifically, our immediate interests lie in comparing [1]'s rectangular central window against the circular windows used in this study. We also wish to probe into understanding the longitudinal effect of adaptation to cybersickness and further investigate this phenomenon across different window sizes by altering our experiment protocol to involve repeated exposures to the same condition (over multiple sessions) in a between-subjects design. This would allow us to more thoroughly investigate how subjects differentially calibrate to sickness based on the amount of blur applied to the rendered images. Our long terms interests in this line of work (static peripheral blurring) lie in understanding the interplay between the position, size, and geometry of the central window in reducing CS.

ACKNOWLEDGMENTS

The authors gratefully acknowledge the participants of the study for their time and efforts.

REFERENCES

[1] Oculus from Facebook. 2018. Oculus Go: Fixed Foveated Rendering. Retrieved from https://developer.oculus.com/documentation/unreal/latest/concepts/unreal-ffr/.

[2] Isayas Adhanom, Nathan Navarro Griffin, Paul MacNeilage, and Eelke Folmer. 2020. The effect of a foveated field-of-view restrictor on VR sickness. In *2020 IEEE Conference on Virtual Reality and 3D User Interfaces (VR)*. IEEE, 645–652. DOI:10.1109/VR46266.2020.00087

[3] Patricia L. Alfano and George F. Michel. 1990. Restricting the field of view: Perceptual and performance effects. *Percept. Motor Skills* 70, 1 (1990), 35–45.

[4] Imtiaz Muhammad Arafat, Sharif Mohammad Shahnewaz Ferdous, and John Quarles. 2018. Cybersickness-provoking virtual reality alters brain signals of persons with multiple sclerosis. In *Proceedings of the IEEE Conference on Virtual Reality and 3D User Interfaces (VR'18)*. IEEE, 1–120.

[5] Benjamin Arcioni, Stephen Palmisano, Deborah Apthorp, and Juno Kim. 2019. Postural stability predicts the likelihood of cybersickness in active HMD-based virtual reality. *Displays* 58 (2019), 3–11.

[6] Erica M. Barhorst-Cates, Kristina M. Rand, and Sarah H. Creem-Regehr. 2016. The effects of restricted peripheral field-of-view on spatial learning while navigating. *PloS One* 11, 10 (2016), e0163785.

[7] Doug A. Bowman, David Koller, and Larry F. Hodges. 1997. Travel in immersive virtual environments: An evaluation of viewpoint motion control techniques. In *Proceedings of the IEEE Annual International Symposium on Virtual Reality*. IEEE, 45–52.

[8] Pulkit Budhiraja, Mark Roman Miller, Abhishek K. Modi, and David Forsyth. 2017. Rotation blurring: Use of artificial blurring to reduce cybersickness in virtual reality first person shooters. Retrieved frrom https://arXiv:1710.02599.

[9] Zekun Cao, Jason Jerald, and Regis Kopper. [n.d.]. Visually-induced motion sickness reduction via static and dynamic rest frames. In *Proceedings of the IEEE Conference on Virtual Reality and 3D User Interfaces (VR'18)*. 105–112.

[10] Kieran Carnegie and Taehyun Rhee. 2015. Reducing visual discomfort with HMDs using dynamic depth of field. *IEEE CG&A* 35, 5 (2015), 34–41.

[11] Sarah S. Chance, Florence Gaunet, Andrew C. Beall, and Jack M. Loomis. 1998. Locomotion mode affects the updating of objects encountered during travel: The contribution of vestibular and proprioceptive inputs to path integration. *Presence* 7, 2 (1998), 168–178.

[12] Yi-Ting Chen, Chi-Hsuan Hsu, Chih-Han Chung, Yu-Shuen Wang, and Sabarish V. Babu. 2019. iVRNote: Design, creation and evaluation of an interactive note-taking interface for study and reflection in VR learning environments. In *Proceedings of the IEEE Conference on Virtual Reality and 3D User Interfaces (VR'19)*. IEEE, 172–180.

[13] Paul DiZio and James R. Lackner. 1997. Circumventing side effects of immersive virtual environments. In *Proceedings of the International Conference on Human-Computer Interaction (HCI'97)*. 893–896.

[14] U.S. DoT. 2003. *Manual on Uniform Traffic Control Devices (MUTCD).* Federal Highway Administration, Washington, DC.
[15] Elham Ebrahimi, Bliss Altenhoff, Leah Hartman, J. Adam Jones, Sabarish V. Babu, Christopher C. Pagano, and Timothy A. Davis. 2014. Effects of visual and proprioceptive information in visuo-motor calibration during a closed-loop physical reach task in immersive virtual environments. In *Proceedings of the ACM Symposium on Applied Perception.* 103–110.
[16] Elham Ebrahimi, Bliss M. Altenhoff, Christopher C. Pagano, and Sabarish V. Babu. 2015. Carryover effects of calibration to visual and proprioceptive information on near field distance judgments in 3D user interaction. In *Proceedings of the IEEE Symposium on 3D User Interfaces (3DUI'15).* IEEE, 97–104.
[17] Yu Fang, Ryoichi Nakashima, Kazumichi Matsumiya, Ichiro Kuriki, and Satoshi Shioiri. 2015. Eye-head coordination for visual cognitive processing. *PloS One* 10, 3 (2015), e0121035.
[18] Yasin Farmani and Robert J. Teather. [n.d.]. Viewpoint snapping to reduce cybersickness in virtual reality. In *Proceedings of the Conference on Graphics Interface (GI'18).* 159–166.
[19] Ajoy S. Fernandes and Steven K. Feiner. [n.d.]. Combating VR sickness through subtle dynamic field-of-view modification. In *Proceedings of the IEEE Symposium on 3D User Interfaces (3DUI'16).* 201–210.
[20] Donald L. Fisher, A. P. Pollatsek, and Abhishek Pradhan. 2006. Can novice drivers be trained to scan for information that will reduce their likelihood of a crash? *Injury Prevent.* 12, suppl. 1 (2006), i25–i29.
[21] John F. Golding. 1998. Motion sickness susceptibility questionnaire revised and its relationship to other forms of sickness. *Brain Res. Bull.* 47, 5 (1998), 507–516.
[22] William LeRoy Heinrichs, Patricia Youngblood, Phillip M. Harter, and Parvati Dev. 2008. Simulation for team training and assessment: Case studies of online training with virtual worlds. *World J. Surg.* 32, 2 (2008), 161–170.
[23] Lawrence J. Hettinger and Gary E. Riccio. 1992. Visually induced motion sickness in virtual environments. *Presence: Teleoper. Virtual Environ.* 1, 3 (1992), 306–310.
[24] Sébastien Hillaire, Anatole Lécuyer, Rémi Cozot, and Géry Casiez. 2008. Depth-of-field blur effects for first-person navigation in virtual environments. *IEEE Comput. Graphics Appl.* 28, 6 (2008), 47–55.
[25] Ian P. Howard and Thomas Heckmann. 1989. Circular vection as a function of the relative sizes, distances, and positions of two competing visual displays. *Perception* 18, 5 (1989), 657–665.
[26] Chih-Fan Hsu, Anthony Chen, Cheng-Hsin Hsu, Chun-Ying Huang, Chin-Laung Lei, and Kuan-Ta Chen. 2017. Is foveated rendering perceivable in virtual reality?: Exploring the efficiency and consistency of quality assessment methods. In *Proceedings of the ACM Conference on Multimedia.* 55–63.
[27] Igroup. 2018. Igroup Presence Questionnaire (IPQ). Retrieved from http://www.igroup.org/pq/ipq/.
[28] Robert S. Kennedy, Norman E. Lane, Kevin S. Berbaum, and Michael G. Lilienthal. 1993. Simulator sickness questionnaire: An enhanced method for quantifying simulator sickness. *Int. J. Aviation Psychol.* 3, 3 (1993), 203–220.
[29] Behrang Keshavarz and Heiko Hecht. 2011. Validating an efficient method to quantify motion sickness. *Human Factors* 53, 4 (2011), 415–426.
[30] B. Keshavarz, H. Hecht, and B. D. Lawson. 2014. Visually induced motion sickness: Causes, characteristics, and countermeasures. In *Handbook of Virtual Environments.* CRC Press, 652–703.
[31] Behrang Keshavarz, Bernhard E. Riecke, Lawrence J. Hettinger, and Jennifer L. Campos. 2015. Vection and visually induced motion sickness: How are they related? *Front. Psychol.* 6 (2015), 472.
[32] Eugenia M. Kolasinski. 1995. *Simulator Sickness in Virtual Environments.* Technical Report. Army research inst for the behavioral and social sciences Alexandria VA.
[33] Joseph J. LaViola Jr. 2000. A discussion of cybersickness in virtual environments. *ACM SIGCHI Bull.* 32, 1 (2000), 47–56.
[34] Tae Min Lee, Jong-Chul Yoon, and In-Kwon Lee. 2019. Motion sickness prediction in stereoscopic videos using 3D convolutional neural networks. *IEEE Trans. Visual. Comput. Graph.* 25, 5 (2019), 1919–1927.
[35] Michael E. McCauley and Thomas J. Sharkey. 1992. Cybersickness: Perception of self-motion in virtual environments. *Presence: Teleoper. Virtual Environ.* 1, 3 (1992), 311–318.
[36] Xiaoxu Meng, Ruofei Du, Matthias Zwicker, and Amitabh Varshney. 2018. Kernel foveated rendering. *Proceedings of the ACM Conference on Computer Graphics and Interactive Techniques* 1, 1 (2018), 5:1–5:20.
[37] Kasra Rahimi Moghadam, Colin Banigan, and Eric D. Ragan. 2020. Scene transitions and teleportation in virtual reality and the implications for spatial awareness and sickness. *IEEE Trans. Visual. Comput. Graph.* 26, 6 (2020), 2273–2287.
[38] Phillip E. Napieralski, Bliss M. Altenhoff, Jeffrey W. Bertrand, Lindsay O. Long, Sabarish V. Babu, Christopher C. Pagano, Justin Kern, and Timothy A. Davis. 2011. Near-field distance perception in real and virtual environments using both verbal and action responses. *ACM Trans. Appl. Percept.* 8, 3 (2011), 1–19.
[39] Tao Ni, Doug A. Bowman, and Jian Chen. 2006. Increased display size and resolution improve task performance in information-rich virtual environments. In *Graphics Interface*, Vol. 2006. 139–146.
[40] Guangyu Nie, Yinan Guo, Yue Liu, and Yongtian Wang. 2017. Real-time salient object detection based on fully convolutional networks. In *Proceedings of the Chinese Conference on Image and Graphics Technologies.* Springer, 189–198.

[41] Guang-Yu Nie, Henry Been-Lirn Duh, Yue Liu, and Yongtian Wang. 2020. Analysis on mitigation of visually induced motion sickness by applying dynamical blurring on a user's retina. *IEEE Trans. Visual. Comput. Graph.* 26, 8 (2020), 2535–2545. DOI: https://doi.org/10.1109/TVCG.2019.2893668

[42] Nahal Norouzi, Gerd Bruder, and Greg Welch. 2018. Assessing vignetting as a means to reduce VR sickness during amplified head rotations. In *Proceedings of the 15th ACM Symposium on Applied Perception (SAP'18)*. 1–8. DOI: https://doi.org/10.1145/3225153.3225162

[43] Nitish Padmanaban, Timon Ruban, Vincent Sitzmann, Anthony M. Norcia, and Gordon Wetzstein. 2018. Towards a machine-learning approach for sickness prediction in 360 stereoscopic videos. *IEEE Trans. Visual. Comput. Graph.* 24, 4 (2018), 1594–1603.

[44] Anjul Patney, Marco Salvi, Joohwan Kim, Anton Kaplanyan, Chris Wyman, Nir Benty, David Luebke, and Aaron Lefohn. 2016. Towards foveated rendering for gaze-tracked virtual reality. *ACM Trans. Graph.* 35, 6 (2016), 179.

[45] Randy Pausch, Thomas Crea, and Matthew Conway. 1992. A literature survey for virtual environments: Military flight simulator visual systems and simulator sickness. *Presence: Teleoper. Virtual Environ.* 1, 3 (1992), 344–363.

[46] Nicholas F. Polys, Seonho Kim, and Doug A. Bowman. 2007. Effects of information layout, screen size, and field of view on user performance in information-rich virtual environments. *Comput. Animat. Virtual Worlds* 18, 1 (2007), 19–38.

[47] James T. Reason. 1978. Motion sickness adaptation: A neural mismatch model. *J. Roy. Soc. Med.* 71, 11 (1978), 819–829.

[48] Lisa Rebenitsch. 2015. Managing cybersickness in virtual reality. *XRDS: Crossroads ACM Mag. Students* 22, 1 (2015), 46–51.

[49] Gary E. Riccio and Thomas A. Stoffregen. 1991. An ecological theory of motion sickness and postural instability. *Ecol. Psychol.* 3, 3 (1991), 195–240.

[50] Craig R. Sherman. 2002. Motion sickness: Review of causes and preventive strategies. *J. Travel Med.* 9, 5 (2002), 251–256.

[51] Nicholas T. Swafford, José A. Iglesias-Guitian, Charalampos Koniaris, Bochang Moon, Darren Cosker, and Kenny Mitchell. 2016. User, metric, and computational evaluation of foveated rendering methods. In *Proceedings of the ACM Symposium on Applied Perception*. ACM, 7–14.

[52] Rohith Venkatakrishnan, Roshan Venkatakrishnan, Reza Ghaiumy Anaraky, Matias Volonte, Bart Knijnenburg, and Sabarish V. Babu. 2020. A structural equation modeling approach to understand the relationship between control, cybersickness and presence in virtual reality. In *Proceedings of the IEEE Conference on Virtual Reality and 3D User Interfaces (VR'20)*. IEEE, 682–691.

[53] Roshan Venkatakrishnan, Rohith Venkatakrishnan, Ayush Bhargava, Kathryn Lucaites, Hannah Solini, Matias Volonte, Andrew Robb, Sabarish V. Babu, Wen-Chieh Lin, and Yun-Xuan Lin. 2020. Comparative evaluation of the effects of motion control on cybersickness in immersive virtual environments. In *Proceedings of the IEEE Conference on Virtual Reality and 3D User Interfaces (VR'20)*. IEEE, 672–681.

[54] Jaye Wald and Steven Taylor. 2000. Efficacy of virtual reality exposure therapy to treat driving phobia: A case report. *J. Behav. Ther. Exper. Psych.* 31, 3–4 (2000), 249–257.

[55] Tim Weiβker, André Kunert, Bernd Frohlich, and Alexander Kulik. [n.d.]. Spatial updating and simulator sickness during steering and jumping in immersive virtual environments. In *Proceedings of the IEEE Conference on Virtual Reality and 3D User Interfaces (VR'18)*. 97–104.

[56] Martin Weier, Thorsten Roth, Ernst Kruijff, André Hinkenjann, Arsène Pérard-Gayot, Philipp Slusallek, and Yongmin Li. 2016. Foveated real-time ray tracing for head-mounted displays. In *Computer Graphics Forum*, Vol. 35. Wiley Online Library, 289–298.

[57] Maxwell J. Wells and Michael Venturino. 1990. Performance and head movements using a helmet-mounted display with different sized fields-of-view. *Optic. Eng.* 29, 8 (1990), 870–878.

[58] Richard Yao, Tom Heath, Aaron Davies, Tom Forsyth, Nate Mitchell, and Perry Hoberman. 2014. Oculus VR best practices guide. *Oculus VR* 4 (2014), 27–35.

Received June 2020; revised August 2020; accepted August 2020